Anomalously low modulus of the interpenetrating-phase composite of Fe and Mg obtained by liquid metal dealloying

I.V. Okulov, Pierre-Antoine Geslin, I.V. Soldatov, H. Ovri, S.-H. Joo, H. Kato

Anomalously low modulus of the interpenetrating-phase composite of Fe and Mg obtained by liquid metal dealloying

I.V. Okulov[a,b]*, P.-A. Geslin[a,c], I.V. Soldatov[d,e], H. Ovri[b], S.-H. Joo[a], und H. Kato[a]

[a]Tohoku University, Institute for Materials Research, Katahira 2-1-1, Sendai 980-8577, Japan
[b]Helmholtz-Zentrum Geesthacht, Institute of Materials Research, Division of Materials Mechanics, 21502 Geesthacht, Germany
[c]ELyTMaX UMI 3757, CNRS – Université de Lyon – Tohoku University, International Joint Unit, Tohoku
[d]Ural Federal University, Institute of Natural Sciences and Mathematics, 620002 Yekaterinburg, Russia
[e]IFW Dresden, Helmholtzstraße 20, D-01069 Dresden, Germany

*Corresponding author. E-mail: okulovilya@yandex.ru. I.V. Okulov is currently working at the University of Bremen.

Abstract

A bulk interpenetrating-phase composite consisting of immiscible Fe and Mg metals is fabricated by liquid metal dealloying. The composite exhibits an anomalously low value of the Young's modulus of 20 ± 3 GPa, when probed in compression. The Young's modulus values obtained from nanoindentation and ultrasonic measurements are, however, significantly higher than that in compression, but still remain lower than theoretical values obtained from the Hashin-Strikman bounds and a micromechanics model. Such a deviation is explained by the weak interfaces between Fe and Mg phases that promote phase boundary sliding upon mechanical loading, leading to a low effective modulus.

Key words: Dealloying; Interpenetrating-phase composite; Low modulus; Immiscible metals; Fe-Mg.

The interpenetrating-phase composites (IPCs) consist of at least two different phases each forming an interconnected network. In addition to their ability to combine several properties at once (e.g. electrical, thermal conductivity, magnetic properties, etc.), IPCs can achieve improved mechanical properties by combining soft ductile and hard phases [1,2]. In the case of isotropic microstructures, IPCs can exhibit a significant deviation of their Young's modulus from the ideal composite properties estimated from the Hashin-Strikman bounds [3]. This phenomenon was observed for various IPCs cases, such as for the 420 stainless/bronze IPC [4], the high-strength Mg-based metallic glass/Iron IPC [5] and the high-damping Mg/TiNi IPC [6]. The modulus reduction in the 420 stainless/bronze IPCs was associated with the presence of pores and the significant residual thermal stresses arising from the mismatch of thermal expansion coefficients of both phases. For the Mg/TiNi IPC possible reasons for the significant modulus reduction have not been discussed. The aforementioned IPCs were fabricated by different methods, i.e., metal infiltration into a porous scaffold [1,6] and additive manufacturing [4]. So, the phenomenon seems to be ubiquitous and independent on the fabrication method.

Recently, Wada et al. demonstrated that the metal/metal IPCs with micro or even nano-scale microstructure can be fabricated by liquid metal dealloying (LMD) [7–9]. This recently developed metallurgical technique enables the fabrication of the non-noble porous materials and IPCs. Successful application of LMD has been reported for the fabrications of many porous materials including Mg [10], Fe [11], stainless steel [11], Ti [12,13], Ti alloys [14] (namely, TiZr [15], TiNb [13,16], TiHf [17], and TiFe [16]), Si [18], Cr [11], and C [19]. The dealloying-based IPCs exhibit a unique bicontinuous microstructure, which is difficult (or even impossible) to achieve using classical metallurgical techniques. The unique microstructure of the dealloying-based IPCs leads to attractive mechanical behavior such high and tunable strength as in the Cu-Ta composites [20].

Strong attention has been brought to the mechanical properties of these dealloying-based IPCs. Recent examples include the development of Cu-Ta composites presenting tunable yield stress controlled by the microstructure size [20] and metal/polymer composites for biomedical applications [13,16,17]. In this work, we focus on the particularly curious case of a dealloying-based IPC consisting of interpenetrating Fe and Mg/rich phases. Interestingly, the Young's modulus values of the composite extracted from a standard compression test are anomalously low. Moreover, other

estimates obtained from more precise methods are still significantly lower than the Hashin–Shtrikman lower bounds. These issues are discussed in the manuscript.

The design of precursor alloys for the liquid metal dealloying is based on the enthalpy of mixture between dissolvent (in our case Mg) and the considered alloying element ($\Delta H^{mix}_{(Mg-element)}$). Elements with a negative value of $\Delta H^{mix}_{(Mg-element)}$, like Ni, are miscible and will be dissolved in Mg during dealloying while elements with a positive $\Delta H^{mix}_{(Mg-element)}$, like Fe, are immiscible in Mg leading to formation of IPCs. The $Fe_{30}Ni_{70}$ (at. %) alloy was designed and dealloyed in liquid Mg in order to form the Fe-Mg interpenetrating-phase composite.

The samples of $Fe_{30}Ni_{70}$ (plates of 1 mm in thickness) for liquid metal dealloying were prepared from pure metals (99.99 %) by arc-melting under argon atmosphere followed by rolling. The plates were dealloyed at 1023 K for 30 min in liquid Mg (about 100 g liquid metal bath was used). Upon dealloying, Ni dissolves selectively in liquid Mg while Fe reorganizes at the Fe/Mg interface, and form a porous structure; liquid Mg further penetrates into the open porosity, pursuing the dealloying process and eventually forming an interpenetrating-phase composite consisting of Mg-rich and Fe-rich phases forms [7,9].

Structural investigation of the Fe-Mg composites was performed by X-ray diffraction in Bragg-Brentano geometry with Cu-Kα radiation (SmartLab, Regaku, Japan). Scanning electron microscopy (SEM, Gemini Ultra 55, Karl Zeiss, Germany) coupled with energy-dispersive X-ray analysis (Bruker, Germany) explored microstructure and composition. The samples for the SEM analysis as well as for the nanoindentation tests were polished using Ion Beam Cross Section Polisher (JEOL CP, JEOL, Japan). The samples with square cross-section (1 mm) and length 2 mm were tested in compression at room temperature and a strain rate of 10^{-4} s^{-1}, using a universal testing device (Z010 TN, Zwick-Roell, Germany). The strain was computed from the relative displacement of the load surfaces, as measured by a laser extensometer (LaserXtens, Zwick). The yield strength of the porous metals and composites was determined at the 0.002 offset strain.

The modulus and hardness of the Fe-Mg composite was additionally measured with nanoindentation tests. These tests were performed with the continuous stiffness measurement (CSM) module of a Nanoindenter XP (Agilent GmbH, Germany) equipped with a Berkovich indenter to a

depth of 5um at a constant strain rate of 0.05/s. The ultrasonic measurements of the Young's modulus were performed using an in-house designed device.

Figure 1 a illustrates the X-ray diffraction patterns of the Fe-Mg composite. The composite consists mainly of two phases, Mg and Fe, as well as a minor amount of Mg_2Ni. The SEM analysis also proves the presence of all three phases detected by X-ray analysis. Figure 1 b shows the elemental distribution in the composite. According to EDX analysis, the bright phase on the SEM image consists of Fe while the darker matrix phase consists mostly of Mg. Additionally, there are regions enriched in Ni, which are overlapping with Mg-rich regions (Fig. 1 b). The Mg_2Ni phase as a part of the eutectic structure is visible on the SEM micrograph (Fig. 1 c). The volume fraction of the Fe phase estimated from the SEM micrographs is about 38 vol%.

Mechanical properties of the Fe-Mg composite are presented in Figure 2. Particularly, the quasi-static mechanical tests of the porous and the composite materials are shown in Figure 2 a. The composite exhibits a good compressive deformability and moderate yield strength of about 100 MPa. Consistent with this good plastic deformability is the pronounced strain-hardening of the composite, which promotes uniform plastic flow.

Unexpectedly for a metallic material, the Young's modulus of the composite obtained from the compressive stress-strain curve (Fig. 2 a) is about 20 ± 3 GPa, which is lower than the values for pure iron and magnesium, namely, 210.5 GPa [21] and 45 GPa [22], respectively. In particular, the value is drastically lower than the lower bound obtained from the Hashin-Shtrikman estimates. To investigate the origin of this unexpected result, complementary tests, using different approaches, including the load-unload response of the materials along the compression test, nanoindentation, and ultrasonic measurements.

The Young's modulus obtained for higher strains during the compression test (reported in Fig. 2.b) are ranging from 40 GPa to 50 GPa, i.e., more than two times higher than in the unstrained case. This large increase occurs at small strains with a value of 40 GPa obtained after only 3% of strain. The ultrasonic measurement yields a notably higher value of Young's modulus as compared with the results of the *prestrained* compression samples, namely, 75 ± 5 GPa.

A plot of average nanoindentation modulus and hardness of the composite and the associated standard deviation, computed from an array of 7 indents are shown in Figure 2 c. Although the

sample was Argon ion-milled in a cross section polisher, the top surface was still uneven because of the preferential milling of the Mg phase. In order to minimize the effect of the surface roughness and to capture a truly uniform response, only data between 3 and 5 µm were analyzed. The modulus and hardness values thus calculated are 63 ± 9 GPa and 0.99 ± 0.08 GPa, respectively.

In addition, to go beyond the Hashin-Shtrinkman bounds and assess the influence of the complex bicontinuous microstructure of the samples on the Young's modulus, the elastic properties of a model bicontinuous structure (Fig. 3) have been estimated using a numerical micromechanics approach. The microstructure considered here (Fig. 3) is obtained from a simple phase-field model for spinodal decomposition of a binary mixture [23]. This approach is commonly used to produce numerical microstructures sharing similar properties (bicontinuity, topological and morphological characteristics, etc.) with the ones obtained experimentally from dealloying [24,25]. Isotropic elastic constants of pure Fe (shear modulus G = 82 GPa and Poisson ratio v = 0.29) and Mg (G = 17 GPa, v = 0.29) are then attributed to both phases and the Young's modulus of the composite is computed by means of a micro-mechanics approach: an external stress is applied to the microstructure and we use a spectral method relying on linear elasticity [26,27] to solve for the strain and stress distribution in the material. The Young's modulus of the structure is then computed from volume average of stresses and strains. The average Young's modulus obtained by our simulation is reported in Figure 3 and fall in between the lower and upper Hashin-Shtrikman bounds.

The low value of the Young's modulus measured by the different experimental techniques can results from defected interfaces in the composite materials. Indeed, Hashin-Shtrikman bounds and our numerical micromechanis approach assume perfect interfaces between Mg and Fe phases that fully transmit stresses from one phase to another. However, the severe thermal treatment occurring during the LMD process and the dissimilar nature of Mg and Fe could lead to the formation of interface defects such as pores and cavities. First, the dealloying temperature is above the melting point of pure Mg leading to the liquid-solid transformation of the Mg phase upon cooling. The volume change associated with the solidification of Mg is 4.2 vol% [22]. Second, the thermal expansion coefficients between both phases (35.4 10^{-6} K^{-1} [21] for Fe and 78 10^{-6} K^{-1} [22] for Mg) differ by about 2.2 times. Both thermal effects lead to significant residual stresses in the different phases. A part of these stresses can be relaxed by the plastic deformation of both phases but it is highly probable that

residual thermal stresses cause debounding of Mg/Fe interfaces or the formation of porosity at the interface, as observed in other IPC [1,2]. An upper bound estimate of this porosity volume can be obtained by considering that all the residual stresses are released by the formation of pores, leading to a volume fraction of pores

$$\varphi_{pores} \approx (\alpha_{VMg} - \alpha_{VFe}) \times \Delta T + \Delta V_{liq/sol}$$

where α_{VMg} and α_{VFe} are volumetric coefficients of thermal expansion of Mg and Fe, respectively; ΔT is the difference between Mg melting point and room temperature; and $\Delta V_{liq/sol}$is the volume change due to solidification of Mg. This estimate yields a total porosity volume 7.4 vol%. As shown in previous work [1,4], such porosity could significantly affect the Young's modulus value of the composite. In addition, the increasing of the Young's modulus value during prestraining of the composite could indirectly indicate the porosity closure. However, such porosity should affect the nano-compression measurement in the same way than the ultrasonic estimate of the Young's modulus, which is not the case in our results. In addition, no pores could be clearly observed on the dealloyed sample by SEM analysis indicating nanoscale size of those pores. Therefore, we presume that the formation of nanoscopic cavities (difficult to observe with SEM) can contribute to the underestimation of Young's modulus by ultra-sonic measurement in respect to theoretical values derived from Hashin-Shtrikman but fails to explain the low values obtained in compression testing.

Another explanation is based on the weak bounding between Mg and Fe phases. The dissimilar nature of the metals can lead to weak interfacial boundaries, promoting sliding of the Fe and Mg phases during the deformation. Finally, the sliding of the phase boundaries yields an anomalously low effective Young's modulus probed in mechanical testing. Due to the micro-meter size of the composite microstructure, the surface area of Fe-Mg interfaces is very large making the influence of this interfacial boundary very important.

The lowering of the Young's modulus value due to the grain boundary sliding effect is supported by our results. The Fe-Mg composite with the perfect interfaces considered in our micromechanics approach yields the highest Young's modulus. The ultrasonic measurement, which should be largely insensitive to the interfacial boundaries sliding, yields the Young's modulus value very similar to the modelled one and between the Hashin-Strikman bounds (Fig. 3). In contrast, the compression test is very sensitive to the sliding effect and demonstrates the lowest Young's modulus. In addition, the

weak interfaces between constituent phases were observed by SEM on the polished surface of a deformed sample.

The *ex-situ* microstructural analysis of the deformed Fe-Mg composite at a low strain value, but already in the plastic regime has not reveal significant phase detachment. However, important microstructural changes have been observed after strain of 0.1 (Fig. 4). The plastic deformation and detachment of the phases are clearly visible on these SEM images. Both Fe and Mg phases are plastically deformed. Particularly, the Figure 4 a reflects the plastic deformation of the Mg matrix by slip while the Figure 4 c exemplifies the plastic deformation of the Fe phase by slip. The most compelling observation is the detachment of Fe and Mg phases shown in Figure 4 b. The observed detachments are located near the Mg_2Ni phase.

In summary, the bulk interpenetrating-phase composite consisting of immiscible Fe and Mg metals was fabricated by liquid metal dealloying from the precursor $Fe_{30}Ni_{70}$ alloy. The composite exhibits an unusual mechanical behavior. Particularly, the Young's modulus value of the composite probed by the compression test is 20 ± 3 GPa what is significantly below those values of the composing metals as individuals. The complementary methods used for the alternative measurements of Young's modulus yields higher values of Young's modulus that are still lower than the Hasin-Shtrikman bounds. The quality of interfaces between Fe and Mg phases seems to be a reason for such an anomalous behavior. The weak bonding between Fe and Mg metals (that are highly immiscible) leads to the phase boundary sliding and, therefore, lowering Young's modulus probed under mechanical loading. In contrast, the ultrasonic measurement being insensitive to this grain boundary sliding yields a Young's modulus value relatively close to the theoretical estimates. This slight discrepancy can be attributed to possible Mg/Fe interface debounding from residual stresses originating from the solidification of the Mg phase and the cooling of the sample.

Composites consisting of immiscible metals, such as in this study, can be produced using powder-based additive manufacturing technologies. Therefore, we strongly believe that our findings will have a strong implication for the design of composite materials, especially, for the additive manufacturing technology, in the nearest future.

Acknowledgements

The funding by the International Collaboration Center, Institute for Materials Research (ICC-IMR), Tohoku University, Japan and the Helmholtz Impuls- und Vernetzungsfonds under Grant number HCJRG-315 are gratefully acknowledged.

List of figures

Figure 1 X-Ray diffraction pattern (a) and secondary electron micrographs together with elemental mapping (b and c) of the Fe-Mg composite fabricated from $Fe_{30}Ni_{70}$ precursor alloy (at. %) by dealloying in liquid Mg at 1023 K for 30 min.

Figure 2 Young's modulus extracted from the load-unloading stress-strain curve probed under compression and plotted as function of strain; (c) Young's modulus and hardness probed by nanoindentation.

Figure 3 The microstructure of the Fe-Mg composite (blue contrast – Fe phase and red contrast – Mg phase) used for the phase field modelling (right panel) and summary of Young's modulus values of the Fe-Mg composite obtain by different methods (left panel). Note: Solid line in right panel is an upper Hashin-Shtrinkman bond and dashed line is a lower Hashin-Shtrinkman bond.

Figure 4 *Ex-situ* SEM micrographs of the Fe-Mg composite after strain of 0.1. (a) Slip bands passing through the Mg phase, marked by arrows; (b) Detachment of the Mg_2Ni and Fe as well as Mg and Fe phases, marked by arrows; (c) Slip bands passing through the Fe phase, marked by arrows.

References

[1] L.D. Wegner, L.J. Gibson, Int. J. Mech. Sci. 42 (2000) 925–942.
[2] M.C. Breslin, J. Ringnalda, L. Xu, M. Fuller, J. Seeger, G.S. Daehn, T. Otani, H.L. Fraser, Mater. Sci. Eng. A 195 (1995) 113–119.
[3] Z. Hashin, S. Shtrikman, J. Mech. Phys. Solids 11 (1963) 127–140.
[4] L.D. Wegner, L.J. Gibson, Int. J. Mech. Sci. 42 (2000) 943–964.
[5] H. Ma, J. Xu, E. Ma, Appl. Phys. Lett. 83 (2003) 2793–2795.
[6] W. Guo, H. Kato, Mater. Lett. 158 (2015) 1–4.
[7] T. Wada, K. Yubuta, A. Inoue, H. Kato, Mater. Lett. 65 (2011) 1076–1078.
[8] I. McCue, B. Gaskey, P.A. Geslin, A. Karma, J. Erlebacher, Acta Mater. 115 (2016) 10–23.
[9] P. Geslin, I. Mccue, J. Erlebacher, A. Karma, Nat. Commun. 6 (2015) 1–19.
[10] I.V. Okulov, S. V Lamaka, T. Wada, K. Yubuta, M.L. Zheludkevich, J. Weissmüller, J. Markmann, H. Kato, Nano Res. (2018).
[11] T. Wada, H. Kato, Scr. Mater. 68 (2013) 723–726.
[12] M. Tsuda, T. Wada, H. Kato, J. Appl. Phys. 114 (2013).
[13] I. V Okulov, J. Weissmüller, J. Markmann, Sci. Rep. 7 (2017) 20.
[14] T. Wada, A.D. Setyawan, K. Yubuta, H. Kato, Scr. Mater. 65 (2011) 532–535.
[15] I.V. Okulov, A.V. Okulov, I.V. Soldatov, B. Luthringer, R. Willumeit-Römer, T. Wada, H. Kato, J. Weissmüller, J. Markmann, Mater. Sci. Eng. C 83 (2018) 95–103.
[16] I.V. Okulov, A.V. Okulov, A.S. Volegov, J. Markmann, Scr. Mater. 154 (2018) 68–72.
[17] A.V. Okulov, A.S. Volegov, J. Weissmüller, J. Markmann, I.V. Okulov, Scr. Mater. 146 (2018) 290–294.
[18] T. Wada, T. Ichitsubo, K. Yubuta, H. Segawa, H. Yoshida, H. Kato, Nano Lett. 14 (2014) 4505–4510.

[19] S.G. Yu, K. Yubuta, T. Wada, H. Kato, Carbon N. Y. 96 (2016) 403–410.
[20] I. McCue, S. Ryan, K. Hemker, X. Xu, N. Li, M. Chen, J. Erlebacher, Adv. Eng. Mater. 18 (2016) 46–50.
[21] W.D. Callister, Materials Science and Engineering: An Introduction, John Wiley & Sons, Inc., New York, 2007.
[22] K.U. Kainer, F. Buch, eds., Magnesium - Alloys and Technology, WILEY-VCH Verlag GmbH & Co. KGaA, Weinheim, 2004.
[23] L.-Q. Chen, Annu. Rev. Mater. Res. 32 (2002) 113–140.
[24] D.A. Crowson, D. Farkas, S.G. Corcoran, Scr. Mater. 56 (2007) 919–922.
[25] X.-Y. Sun, G.-K. Xu, X. Li, X.-Q. Feng, H. Gao, J. Appl. Phys. 113 (2013) 023505.
[26] J.C. Michel, H. Moulinec, P. Suquet, Comput. Methods Appl. Mech. Eng. 172 (1999) 109–143.
[27] S.Y. Hu, L.Q. Chen, Acta Mater. 49 (2001) 1879–1890.

***Graphical Abstract**

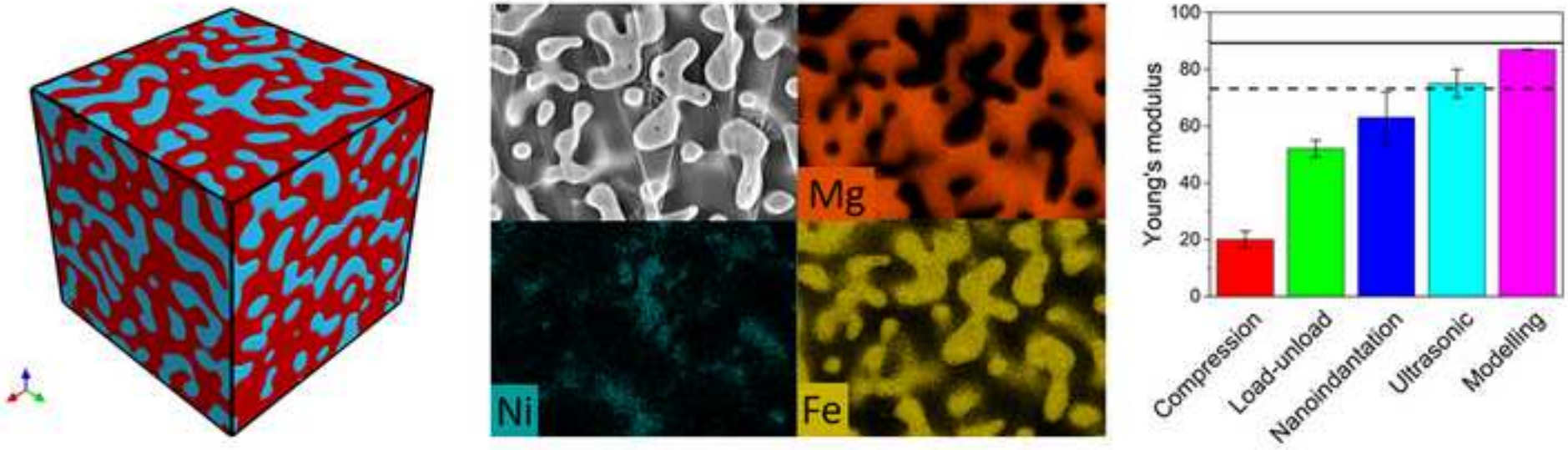

Figure 1

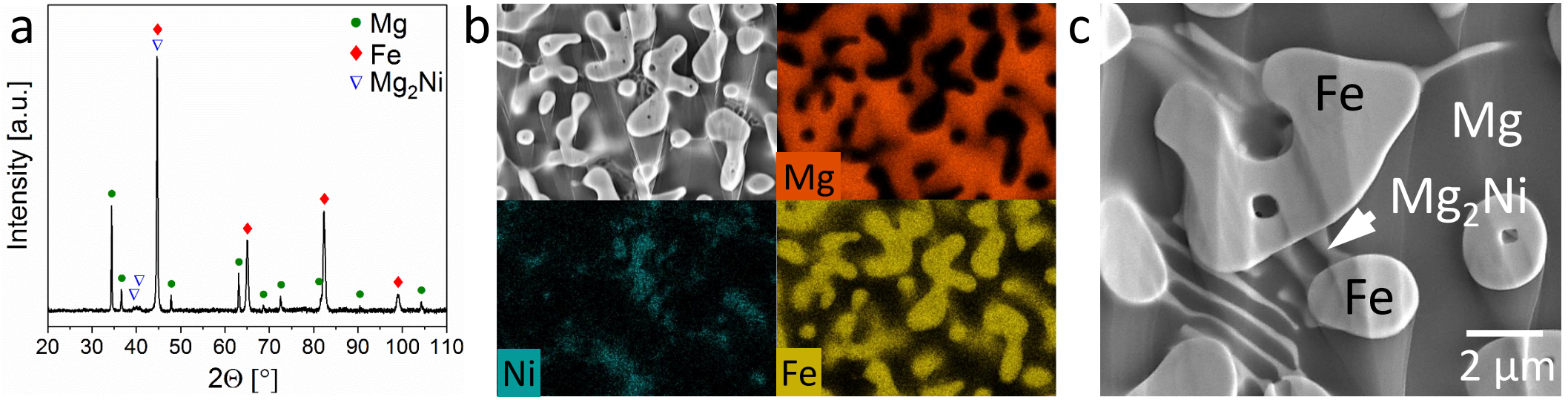
a
Mg
Fe
Mg2Ni
Intensity [a.u.]
20 30 40 50 60 70 80 90 100 110
2Θ [°]
b
Mg
Ni
Fe
c
Fe
Mg
Mg2Ni
Fe
2 µm

Figure 2

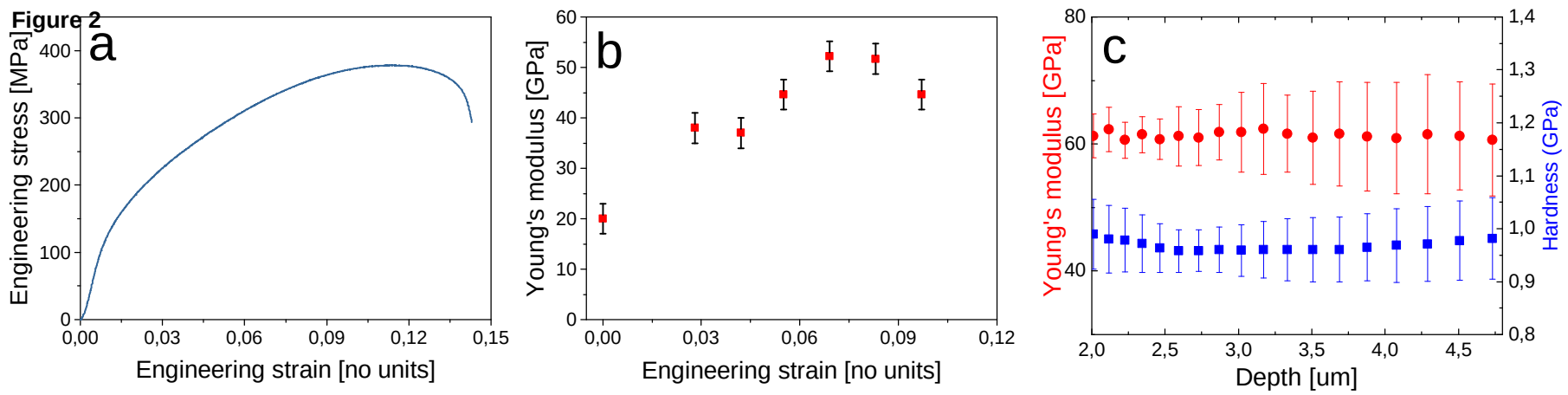
a
Engineering stress [MPa]
0
100
200
300
400
0,00
0,03
0,06
0,09
0,12
0,15
Engineering strain [no units]
b
Young's modulus [GPa]
0
10
20
30
40
50
60
0,00
0,03
0,06
0,09
0,12
Engineering strain [no units]
c
Young's modulus [GPa]
40
60
80
Hardness (GPa)
0,8
0,9
1,0
1,1
1,2
1,3
1,4
2,0
2,5
3,0
3,5
4,0
4,5
Depth [um]

Figure 3

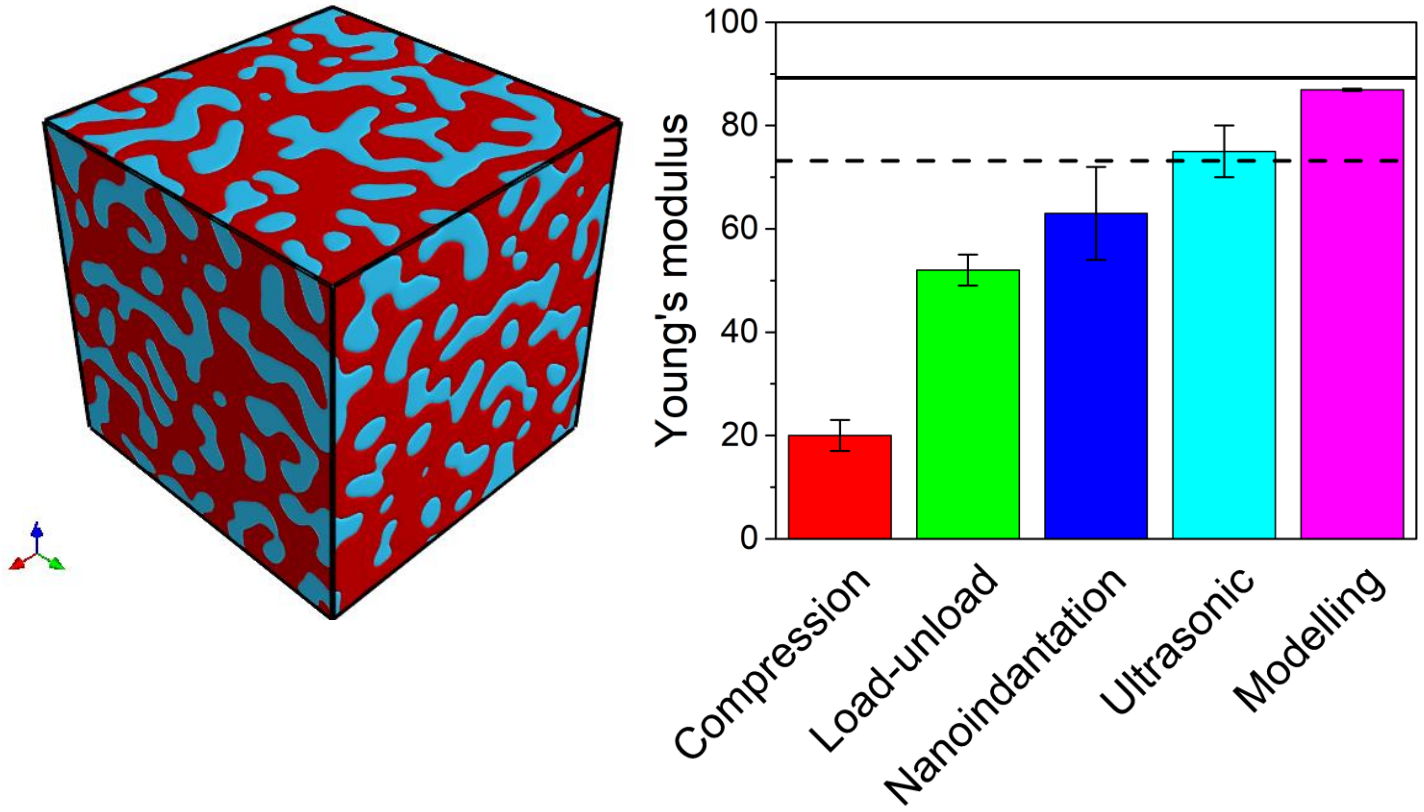
100
80
60
40
20
0
Young's modulus
Compression
Load-unload
Nanoindantation
Ultrasonic
Modelling

Figure 4